Everest Advances in Science and Technology (EAST) Vol. 2, No. 1, 2026
ISSN: 3102-0410 (Print), 3102-0429 (Online)
DOI: 10.3126/east.v2i1.98628

Estimation of Suspended Sediment Load and Spatial Distribution of Sediment Yield in the Marsyangdi River Basin, Nepal

SADIKSHYA GHIMIRE[1*], RAM KRISHNA REGMI[2]

Abstract. Himalayan river basins are characterized by exceptionally high sediment loads driven by active tectonics, glacial influence, steep terrain, and intense monsoon precipitation, yet quantitative estimates of spatially distributed sediment generation remain scarce in Nepal. This gap constrains the sustainable planning and operation of run-of-river hydropower projects, where excessive sediment loads increase turbine abrasion, maintenance costs, and production losses. This study applied the Soil and Water Assessment Tool (SWAT) to estimate sediment yield and sediment concentration in the Marsyangdi River Basin, Nepal, a 2,944 km^2 glaciated tributary of the Gandaki River system hosting three operational run-of-river hydropower stations with a combined installed capacity of 189 MW. The model was calibrated for 2012–2014 and validated for 2015, reproducing streamflow with very good performance (NSE = 0.864, R^2 = 0.874 in calibration; NSE = 0.830, R^2 = 0.867 in validation) and sediment load with satisfactory performance (NSE = 0.556, R^2 = 0.608 in calibration; NSE = 0.516, R^2 = 0.617 in validation). Simulation for 2012–2024 indicated that about 89% of total basin sediment generation originates from five southern sub-basins characterized by higher orographic precipitation, whereas northern rain-shadow sub-basins contribute only marginally. Average annual sediment export at the basin outlet was estimated at 9.42 Mt/yr, with mean sediment concentration of 1,385 mg/L. About 73% of the annual sediment load occurred during the monsoon months, with concentrations exceeding the 1,500 ppm operational threshold on 95 days a year, highlighting a distinct period of elevated hydropower operational risk and the need for targeted monitoring and watershed management.

Keywords: Hydropower, Marsyangdi River Basin, Monsoon, Nepal, Sediment Concentration, Sediment Yield, Soil and Water Assessment Tool, Watershed Management

[1], [2] Institute of Engineering, Pulchowk Campus, Lalitpur, Nepal
E-mail: 080mshpe015.sadikshya@pcampus.edu.np
* Corresponding author

Manuscript received: 16 March 2026; Revised: 10 June 2026; Accepted: 15 July 2026.

1. INTRODUCTION

Sediment transport is a distinguishing hydrologic and geomorphic feature of the Himalayan rivers. In Nepal, high sediment yield occurs due to the effect of active tectonics, steep topography, strong seasonality of monsoonal precipitation, and frequent slope failures. Moreover, orographic gradients enhance rainfall and erosion processes within short spatial extents. These factors make sediment load generation very variable in space and time. As a consequence, basins in Nepal possess among the highest sediment contents in fluvial channels all over the world [1, 2].

This sedimentation process is not only an important geomorphologic factor but also a serious problem for infrastructure development. Sediment affects river geomorphology, storage capacity, and ecological balance, hydropower stations are affected by abrasion of turbines, clogging of waterways, increased need for maintenance, and decreased efficiency. These problems become especially acute for the run-of-river hydropower plants, because in this type of plants sediment-rich water passes through diversion structures and turbine during the monsoon period [3]. Therefore, reliable estimation of sedimentation becomes crucial for hydropower development in mountainous regions, like central Nepal.

However, quantification of sediment load in Himalayan catchments is difficult task due to a lack of continuous measurements and seasonal hysteresis in sediment concentration relative to streamflow. It means that sediments cannot be evaluated based on streamflow due to the modulation of the runoff partitioning, hillslope contributions, and seasonal storage-release processes [4]. It results in deficiency of basin scale assessments of sediment generation and sediment sources in Nepal despite the urgency of these problems [5].

Hydrologic process-based modeling can become a good solution to these problems. Several modeling tools are available; however, Soil and Water Assessment Tool (SWAT) becomes widely used for modeling watersheds hydrology, sediment dynamics, and the effect of land management practices. This physically based semi-distributed model incorporates the heterogeneity of the basin through sub-basins and hydrologic response units, and becomes very suitable for basin-scale modeling [6, 7]. Some previous researches showed that SWAT gives good estimations of hydrological variables in Himalayan and Nepalese catchments. Also, it was proved that the model is applicable for the sediment source identification without extensive field data [8].

Marsyangdi River Basin becomes a good object for such a study because this catchment includes 2,944 km^2 glaciated basin and is a part of the Gandaki River system. The upper Marsyangdi River supports three operational run-of-river hydropower stations: Upper Marsyangdi A, Middle Marsyangdi, and Marsyangdi with total installed capacity of 189 MW. The sediment affects not only downstream hydropower performance but also the upstream landscape processes. Thus, a spatially explicit estimate of sediment generation is important in this basin.

The present study applies SWAT to the Marsyangdi River Basin: (1) To estimate sediment load and sediment concentration, (2) To identify the dominant sediment-contributing sub-basins and (3) To provide a basin-scale sediment framework relevant to watershed management and hydropower sustainability.

2. STUDY AREA

Marsyangdi River Basin, shown in Fig. 1, is a major tributary of the Gandaki River system. It is located in central Nepal and it forms an important hydropower potential catchment of Nepal. For the study, the basin was delineated with outlet point at the Bhakundebesi gauging station (Station 439.35), giving a catchment area of 2,943.36 km^2. The basin shows a strong topographic and climatic variability as the elevation extends from 718 m to 7,925 m above sea level. The Marsyangdi

River originates from the confluence of the Jharsang Khola and Khangsar Khola above 3,600 m northwest of the Annapurna range and flows for about 150 km before joining the Trishuli River at Mugling. Therefore, the basin provides a suitable setting for investigating hydrological and sediment dynamics in a monsoon-influenced Himalayan catchment.

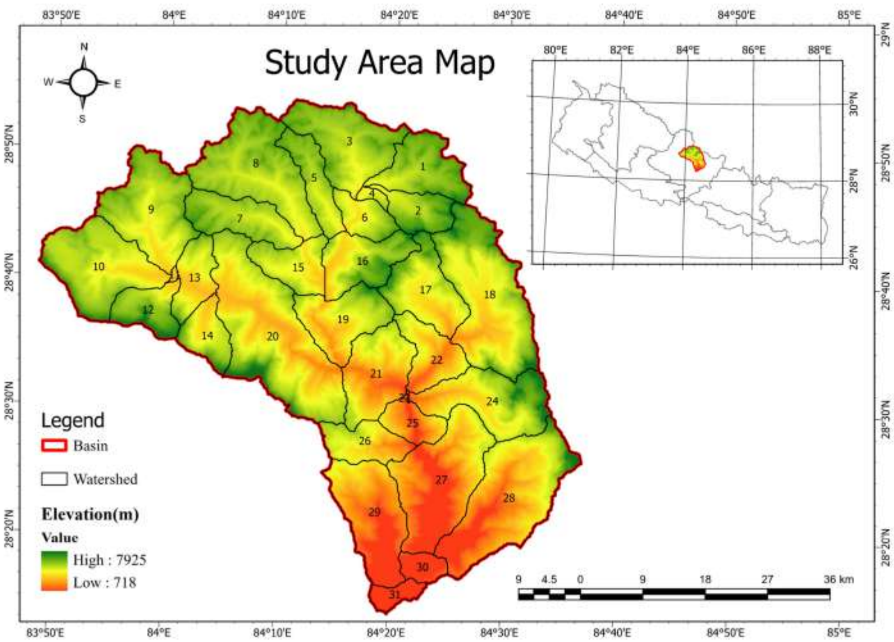

Figure 1. Study area map of Marsyangdi River Basin.

3. MATERIALS AND METHODS

3.1. DATA SOURCES AND PREPARATION.

3.1.1. *TOPOGRAPHIC DATA.* The Digital Elevation Model (DEM) data used in this study was obtained from the Shuttle Radar Topography Mission (SRTM) with resolution of 30 m. It provides a detailed representation of the terrain and allows for thorough hydrological modeling.

3.1.2. *LAND USE AND LAND COVER DATA.* Land use and land cover (LULC) data were obtained from the ICIMOD 2010 land cover map of Nepal. Fig. 2 represents the major land cover types of the Marsyangdi catchment and provides the spatial basis for representing vegetation cover, agricultural land, barren surfaces, snow/glacier areas, and water bodies in the model. Table I summarizes the corresponding distribution of land use classes in terms of area and percentage. LULC was used to define SWAT land cover classes for Hydrological Response Unit (HRU) generation.

3.1.3. *SOIL DATA.* Soil information was obtained from the Soil and Terrain Database (SOTER) for Nepal (Fig. 3), available through the ISRIC data hub. It was used to assign the soil physical properties required for SWAT simulation. The Marsyangdi catchment contains seven major soil groups. Gelic Leptosols occupies the largest share of the basin, indicating widespread shallow and weakly developed mountain soils typical of steep high-altitude terrain. Table II summarizes the distribution of the major soil categories in terms of area and percentage.

Table 1. Land use distribution in the Marsyangdi River Basin

Land use	**Code**	**Area (km^2)**	**% of Area**
Forest	FRST	438.343	14.892
Shrubland	SHRB	133.4868	4.535
Grassland	GRAS	683.4466	23.219
Agricultural Land	AGRL	42.0917	1.43
Barren Land	BARR	487.9701	16.578
Waterbodies	WATB	13.8637	0.471
Snow / Glacier	ICES	1142.5117	38.815
Urban Area	URBN	1.76608	0.06

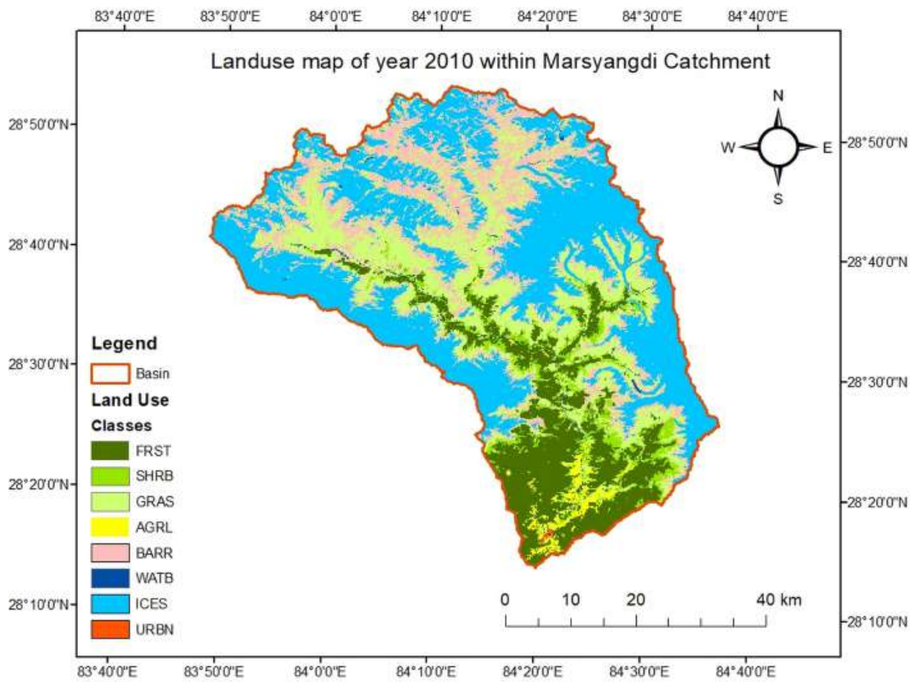

Figure 2. Land Use and Land Cover map of Marsyangdi Basin.

Table 2. Distribution of soil type in the Marsyangdi Catchment

Soil Type	**Area (km^2)**	**Area (%)**
Eutric REGOSOLS	340.97	11.584
Gelic LEPTOSOLS	2093.84	71.135
GLACIER	29.99	1.019
Humic CAMBISOLS	407.34	13.839
Eutric CAMBISOLS	49.36	1.677
Chromic CAMBISOLS	19.16	0.651
Gleyic CAMBISOLS	2.796	0.095

3.1.4. *METEOROLOGICAL DATA.* The daily precipitation data for stations around the vicinity of the study area are obtained from Department of Hydrology and Meteorology (DHM) (Table III) for year 2010 to 2019. Six meteorological stations were selected to provide comprehensive coverage (Fig. 4). The selection of these stations was supported by Thiessen polygon analysis.

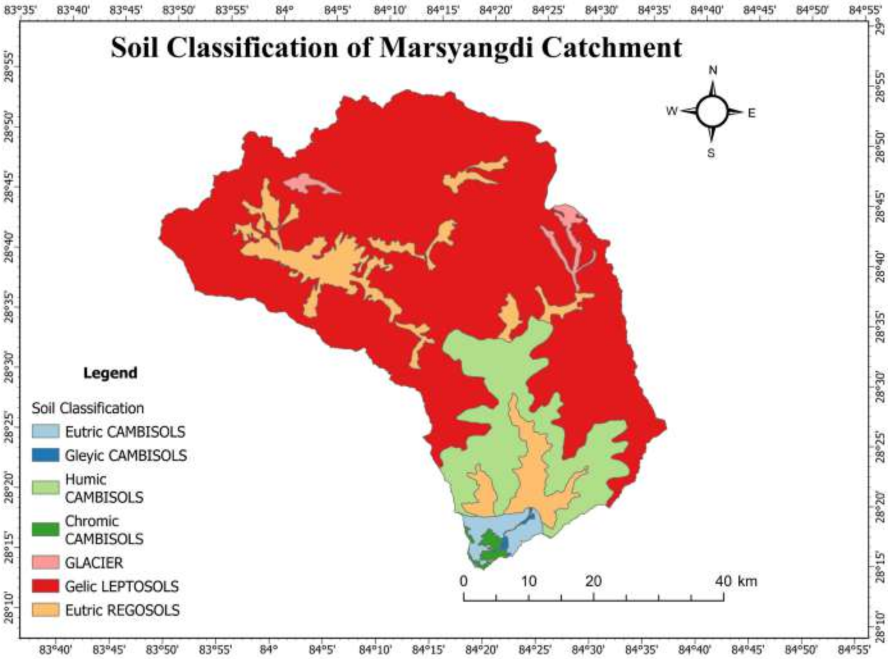

FIGURE 3. Soil classification map of the Marsyangdi River Basin.

3.1.5. *HYDROLOGICAL DATA.* Daily discharge data is obtained from DHM. The location of the gauging station is shown in Fig. 4. The analysis used daily discharge record from year 2010 to 2015 for the station 439.35 (Bhakundebesi station).

3.1.6. *SEDIMENT DATA.* Observed suspended sediment concentration (SSC) data was obtained from DHM at the Bhakundebesi station. The data was intermittent and for the year 2012–2015. SSC observations were available for only 694 of 1,461 days (47.5% coverage). Monsoon-season availability (371 of 488 June–September days, 76%) was relatively better, but high-flow event representation above 300 m^3/s was limited. To obtain a continuous daily SSC series for analysis, the missing sediment data were estimated using an optimization-based suspended sediment rating approach following [9]. This approach was adopted to reduce bias in sediment estimation and to better represent long term sediment variability under intermittent observations.

TABLE 3. Data Collection

Type of data	**Source**	**Spatial/Temporal Resoluti**
DEM	SRTM, USGS `https://earthexplorer.usgs.gov`	30 m × 30 m
Land Cover	ICIMOD Land Cover map 2010	30 m × 30 m
Soil Map	ISRIC, SOTER (Dijkshroon and Huting, 2009)	1:1 million
Climatic (Daily Precipitation)	DHM, Nepal	Station number: 802, 806, 820
Daily Discharge Data	DHM, Nepal	Station number: 439.35
Sediment Concentration	DHM, Nepal	Station number: 439.35

3.2. **SWAT MODEL DESCRIPTION.** SWAT is a semi distributed, process based and continuous time watershed model that simulates hydrology and sediment transport at the level of sub-basins and HRUs. In SWAT, basin hydrology is governed by the water balance equation (1),

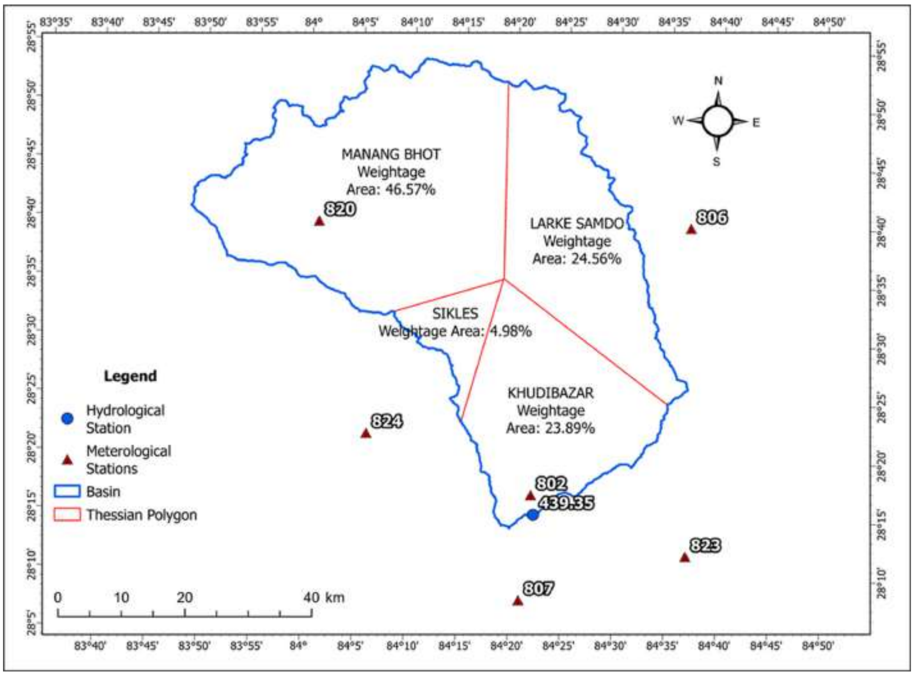

FIGURE 4. Basin boundary at Station 439.35 with meteorological and hydrological stations near the basin, that represent its hydrology.

which forms the basis for runoff generation and subsequent sediment transport:

$$SW_t = SW_0 + \sum_{i=1}^{t} (R_{day} - Q_{surf} - E_a - W_{seep} - Q_{gw}) \quad (1)$$

where SW_t is the final soil water content, SW_0 is the initial soil water content, R_{day} is precipitation, Q_{surf} is surface runoff, E_a is evapotranspiration, W_{seep} is percolation from the soil profile and Q_{gw} is return flow.

In SWAT, sediment yield from each HRU is estimated using the Modified Universal Soil Loss Equation (MUSLE), in which runoff energy replaces rainfall erosivity [10].

The MUSLE formulation used in SWAT is:

$$Sed = 11.8\,(Q_{surf} * q_{peak} * A_{hru})^{0.56} * K_{USLE} * C_{USLE} * P_{USLE} * LS_{USLE} * CFRG \quad (2)$$

where, Sed is sediment yield from the HRU, Q_{surf} is surface runoff volume, q_{peak} is peak runoff rate, A_{hru} is HRU area, K_{USLE} is the soil erodibility factor, C_{USLE} is the cover-management factor, P_{USLE} is the support-practice factor, LS_{USLE} is the topographic factor and $CFRG$ is the coarse fragment factor. Thus, sediment generation in SWAT is controlled by runoff magnitude, peak flow, land cover, soil properties and slope conditions.

Previous applications have also shown that SWAT can perform satisfactorily in Nepalese mountain basins, including the Karnali and West Rapti basins, supporting its use for basin-scale hydrological and sediment-related assessment in data-scarce Himalayan catchments (Dhami, Himanshu, Pandey, and Gautam, 2018; Shrestha and Thakuri, 2025).

[10] further states that erosion and sediment yield are estimated for each HRU using MUSLE and sediment generated on hillslopes is then released to and routed through the channel network. MUSLE uses runoff as the erosive driver rather than rainfall. Therefore, it has improved sediment-yield prediction, removes the need for sediment delivery ratios and allows estimation at the event scale. This makes the approach suitable for monsoon dominated basins where runoff is the main driver of suspended sediment mobilization. Sediment focused SWAT applications in the Himalayan region further support the use of SWAT for estimating sediment yield and identifying dominant source areas under data-limited conditions [5].

3.3. SWAT MODEL SETUP.

3.3.1. *WATERSHED DELINEATION.* The Marsyangdi watershed was delineated in ArcSWAT using the 30 m DEM, with the basin outlet fixed at the Bhakundebesi gauging station. Stream network extraction and sub-basin definition were performed after standard DEM preprocessing. A threshold drainage area of 500 ha was adopted for stream initiation, which discretized the basin into 31 sub-basins. This sub-basin framework was used to represent the spatial variability of hydrological and sediment processes across the catchment.

3.3.2. *HRU DEFINITION.* Hydrologic Response Units (HRUs) were generated by overlaying land use, soil, and slope layers within each sub-basin. Slope was classified into five classes: 0–5%, 5–15%, 15–30%, 30–45%, and >45%. All unique combinations of land use, soil, and slope resulted in 108 HRUs. This discretization allowed runoff generation and sediment yield to be simulated at a spatially distributed level.

3.3.3. *SIMULATION PERIOD AND TIME STEP.* The model was run at a daily time step using the prepared spatial layers and hydro-meteorological inputs. The simulation period covered 2012–2024, with an initial warmup period used to stabilize soil moisture, groundwater storage, and related state variables before model evaluation. Observed discharge and suspended sediment data at the basin outlet were later used for calibration during 2012–2014 and validation in 2015.

3.4. CALIBRATION AND VALIDATION.

3.4.1. *CALIBRATION APPROACH.* Model calibration and validation were carried out using the SWAT Calibration and Uncertainty Program (SWAT-CUP) with the Sequential Uncertainty Fitting algorithm (SUFI-2), which is applied for SWAT parameter optimization and uncertainty analysis in Himalayan basins. Calibration was performed at a daily time step using observed discharge and SSC data at the Bhakundebesi outlet station. Following standard SWAT practice, streamflow was calibrated first to establish a reliable hydrological response, after which sediment-related parameters were adjusted using the calibrated hydrological simulation as the basis for sediment generation and routing.

The model was run for the period 2012–2015, with an initial warm-up period to stabilize model state variables. Calibration was conducted for 2012–2014 and validation was performed for 2015 using an independent dataset.

3.4.2. *SELECTION OF CALIBRATION PARAMETERS.* Calibration parameters were selected based on their physical relevance to runoff generation, groundwater response, snowmelt processes, channel routing and sediment generation in steep Himalayan catchments, together with guidance from previous SWAT applications and published literature [5, 8, 11, 12]. For streamflow calibration, parameters influencing surface runoff, baseflow, groundwater delay, soil water processes, snowmelt, elevation-related climatic variation and channel flow routing were considered, consistent with SWAT-based hydrological studies in mountainous and Nepalese river basins [8, 12]. For sediment calibration, parameters related to soil erodibility, support practice, cover-management, channel re-entrainment and sediment routing were emphasized following sediment-focused SWAT applications in Himalayan catchments [5]. Parameter ranges were initially assigned from literature and SWAT documentation and were progressively refined through successive SUFI-2 iterations, following the calibration and uncertainty framework of SWAT-CUP/SUFI-2 [11]. The final set of calibration parameters and their fitted ranges are presented in Table IV and Table V.

3.4.3. *PARAMETERS EVALUATION METRICS.* Model performance was evaluated by comparing observed and simulated data, discharge and suspended sediment concentration, using the Nash–Sutcliffe Efficiency (NSE), coefficient of determination (R^2) and percent bias (PBIAS) given by (3), (4) and (5) respectively. NSE was used to assess the agreement between observed and simulated time series. R^2 was used to evaluate the strength of association between observed and simulated values. PBIAS was used to quantify the average tendency of the model to overestimate or underestimate observations.

The majority of sediment transport in the basin occurs during high flow monsoon conditions and these periods are most relevant to sediment management and hydropower operations. Thus, the model performance for suspended sediment was also interpreted with particular emphasis on monsoon-period observations.

$$NSE = 1 - \frac{\sum_{i=1}^{n} \left(Q_{sim} - Q_{obs}\right)^2}{\sum_{i=1}^{n} \left(Q_{sim} - \bar{Q}_{obs}\right)^2} \tag{3}$$

$$PBIAS = \frac{\sum_{i=1}^{n} \left(Q_{obs} - Q_{sim}\right)}{\sum_{i=1}^{n} Q_{obs}} \times 100\% \tag{4}$$

$$R^2 = \left[\frac{n \sum Q_{obs} Q_{sim} - \sum Q_{obs} \sum Q_{sim}}{\sqrt{\left(n \sum Q_{obs}^2 - \left(\sum Q_{obs}\right)^2\right)\left(n \sum Q_{sim}^2 - \left(\sum Q_{sim}\right)^2\right)}} \right]^2 \tag{5}$$

Table 4. Streamflow Calibration Parameters and Ranges Used in SWAT-CUP

Parameters	**Min**	**Max**
R__CN2.mgt	-0.2	0.2
V__ALPHA_BF.gw	0	1
V__GW_DELAY.gw	0	100
R__SOL_Z.sol	-0.25	0.25
R__SOL_K.sol	-0.8	0.8
R__SOL_AWC.sol	-0.2	0.4
V__GW_REVAP.gw	0	0.2
V__OV_N.hru	0	30
V__CH_N2.rte	0	0.3
V__CH_K2.rte	-0.01	500
V__SFTMP.bsn	-5	5
V__SMFMN.bsn	0	10
V__SMFMX.bsn	0	10
V__SNOCOVMX.bsn	0	500
V__PLAPS.sub	0	200
V__TLAPS.sub	-10	10
V__EPCO.bsn	0	1

Table 5. Sediment Calibration Parameters and Ranges Used in SWAT-CUP

Parameters	**Min**	**Max**
V__PRF_BSN.bsn	0.03	0.7
V__ADJ_PKR.bsn	0.5	2
R__USLE_K.sol	-0.15	0.3
R__USLE_P.mgt	-0.3	0.25
V__LAT_SED.hru	500	30000
V__SPCON.bsn	0.0025	0.02
V__SPEXP.bsn	1	2
V__CH_COV1.rte	0	1
V__CH_COV2.rte	0	1

4. RESULTS

4.1. SWAT MODEL PERFORMANCE.

4.1.1. *STREAMFLOW PERFORMANCE.* Daily streamflow at the Marsyangdi basin outlet simulation in SWAT produced very good performance in both calibration and validation. As shown in Table 6, during calibration (2012–2014), the model achieved NSE = 0.8641, R^2 = 0.8739, and PBIAS = +4.37%, and in validation for 2015 produced NSE = 0.8301, R^2 = 0.8678, and PBIAS = -9.42%. According to the evaluation criteria of Moriasi et al., 2007, these results indicate that SWAT captured the basin hydrology reliably. The model reproduced the overall seasonal hydrograph pattern, the monsoon changes, peak-flow period and recession behavior well (Fig. 5).

4.1.2. *SEDIMENT LOAD PERFORMANCE.* Sediment simulation was more moderate, within the satisfactory range for basin-scale application. As shown in Table 6, SWAT achieved NSE = 0.5560, R^2 = 0.6080, and PBIAS = +14.4% in calibration and produced NSE = 0.5160, R^2 = 0.6170, and PBIAS = +24.2% in validation. Thus the model reproduced the broad seasonal pattern of sediment transport, especially the concentration of sediment delivery during the monsoon months, but with greater uncertainty than streamflow simulation. SWAT tends to smooth the sharp monsoon sediment peaks (Fig. 5b) and was less effective in reproducing high-magnitude sediment events. However, the performance is adequate for annual, seasonal and spatial sediment assessment within the basin.

Table 6. SWAT Model Calibration and Validation Performance Summary (Moriasi et al. 2007 Criteria)

Parameter	**Flow Calibration**	**Flow Validation**	**Sed Calibration**	**Sed Validation**
NSE	0.864	0.830	0.556	0.516
R^2	0.874	0.867	0.608	0.617
PBIAS (%)	+4.37	-9.42	+14.4	+24.2
Rating	Very Good	Very Good	Satisfactory	Satisfactory

4.2. **SEDIMENT YIELD AND SPATIAL DISTRIBUTION.** The SWAT model estimated an average annual sediment export of 9.42 Mt/yr at the Marsyangdi basin outlet over the simulation period 2012–2024. The spatial distribution of model-produced sediment yield was highly uneven across the basin. Sediment generation was concentrated in a limited number of southern and southeastern sub-basins rather than being uniformly distributed throughout the catchment (Fig. 8). Sub-basins 28, 27, 21, 29 and 26 together contributed about 89% and the remaining 26 sub-basins contributed only about 11% of the total basin sediment generation (Table VII). This indicates that sediment yield in the Marsyangdi basin is strongly concentrated in a small number

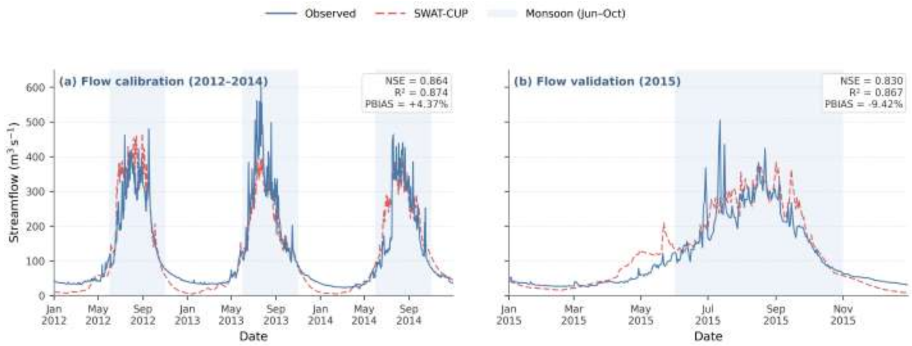

FIGURE 5. Observed and SWAT-simulated daily streamflow during calibration and validation at the basin outlet.

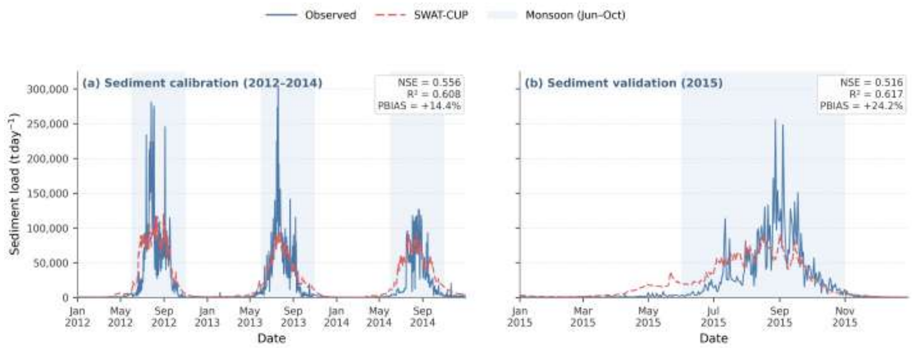

FIGURE 6. Observed and SWAT-simulated daily streamflow and sediment load during calibration and validation at the basin outlet.

of hotspot areas.

The distribution of average annual precipitation and sediment yield is shown in Fig. 6a and Fig. 6b respectively. The wetter part of the basin is concentrated mainly in the southern and southeastern sub-basins, while the northern and northwestern parts of the basin receive comparatively lower precipitation. The major sediment-contributing sub-basins, particularly 28, 27, 21, 29, and 26, lie within the wetter southern sector. Whereas many of the lower-yield northern and northwestern sub-basins correspond to the lower-precipitation zone. This indicates that the dominant sediment generating areas are concentrated within the monsoon-exposed southern part of the basin.

TABLE 7. Major Sediment-Contributing Sub-Basins and Cumulative Contribution to Total Basin Sediment Generation

Rank	Sub-basin	Individual Contribution %	Cumulative %
1	28	23%	23%
2	27	22%	45%
3	21	17%	62%
4	29	16%	78%
5	26	11%	89%

Although the precipitation pattern provides an important basis for understanding the broad distribution of sediment yield, some eastern sub-basins with relatively high precipitation do not show the similar spatial correspondence with high sediment yield. Thus, precipitation alone cannot completely explain the observed spatial variability. Therefore, additional catchment controls are likely involved in determining the intensity of sediment generation across individual sub-basins.

The model consistently identifies a limited number of dominant sediment-source sub-basins within the watershed. This spatial concentration is one of the main quantitative findings of the study.

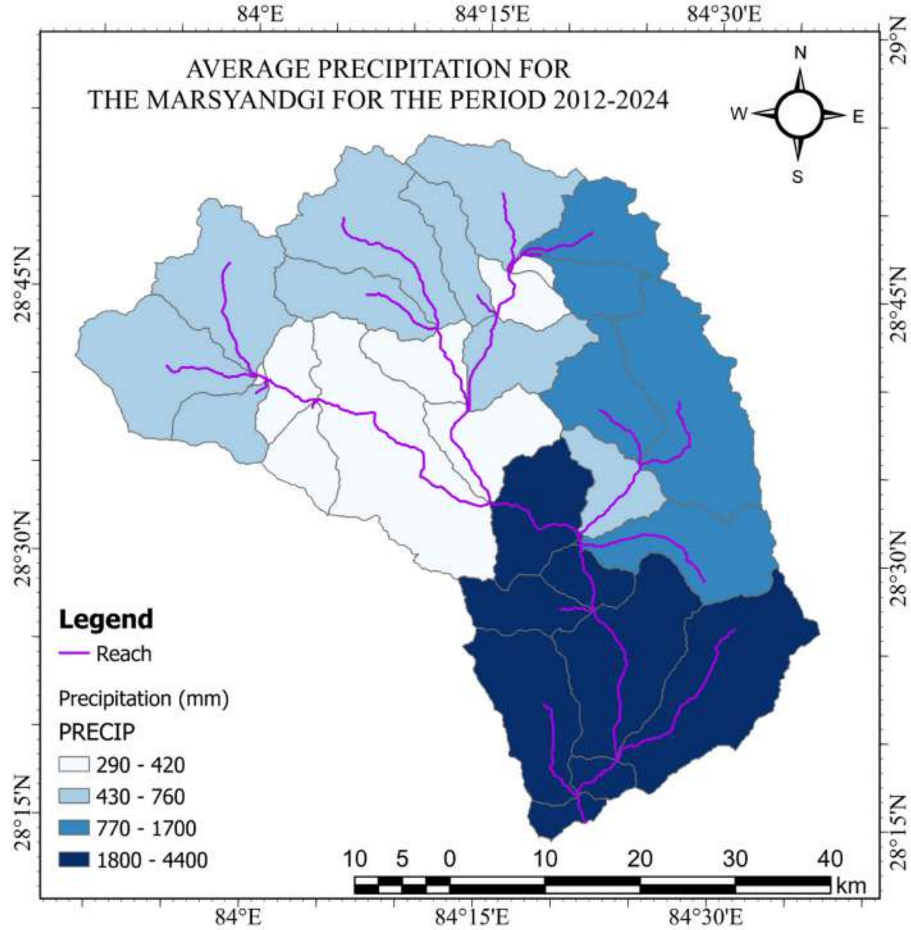

FIGURE 7. Average annual precipitation in the Marsyangdi Basin for the period 2012–2024.

4.3. **SUSPENDED SEDIMENT CONCENTRATION AND HYDROPOWER OPERATIONAL RISKS.** The mean annual sediment concentration over 2012–2024 was 1,385 mg/L at the basin outlet, indicating high-sediment conditions in the basin. As shown in Fig. 7 and Table 8, sediment concentration follows a strong seasonal pattern, remaining low during the dry months but rising sharply with the onset of the monsoon. The sediment transport is heavily concentrated within the monsoon season. Monthly average concentration increased to 4,500 mg/L in June, peaked at 5,200 mg/L in July, remained high at 4,800 mg/L in August, and declined to 2,800 mg/L in September. In contrast, monthly average concentrations during the dry months remained minimum with the lowest values occurring between December and March.

Fig. 8 shows that average sediment concentration is spatially heterogeneous across the basin. The highest reach-scale concentrations concentrated in the southern and southeastern parts of the

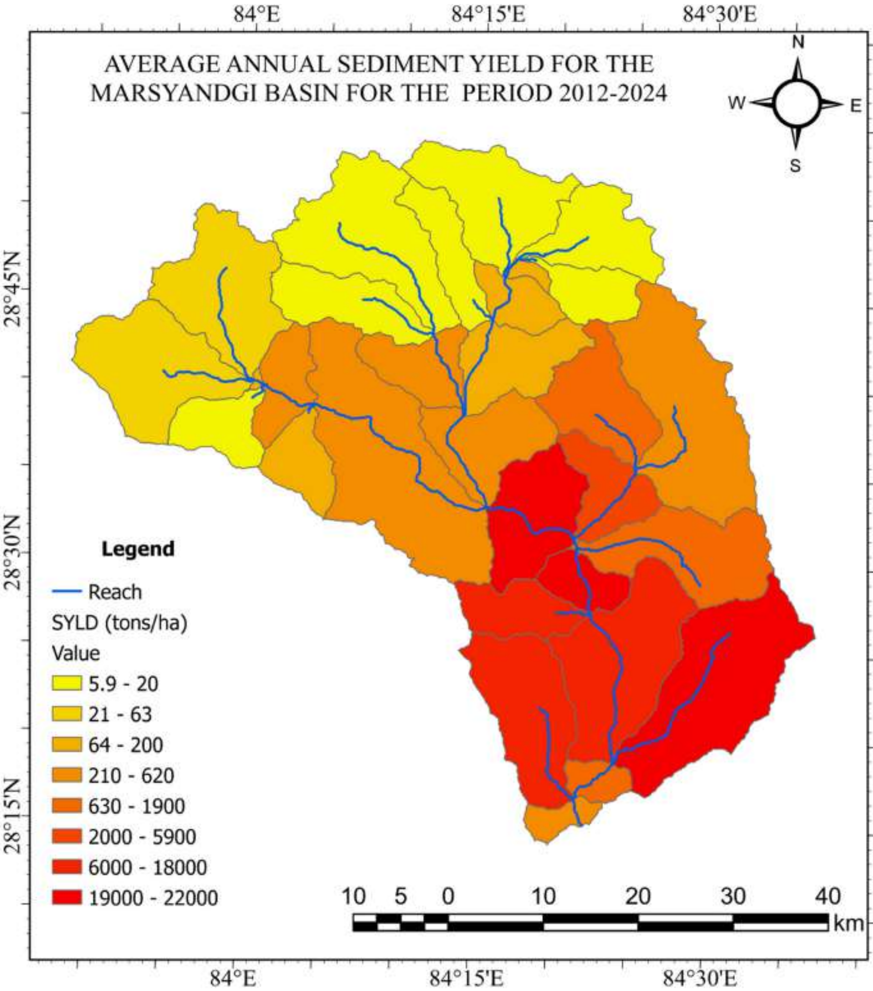

FIGURE 8. Average annual sediment yield in the Marsyangdi Basin for the period 2012–2024.

catchment.

TABLE 8. Monthly Average Discharge, Sediment Concentration, Annual Sediment Share, and Operational Risk Level at the Marsyangdi Basin Outlet (2012–2024)

Month	Avg Q (m^3/s)	Avg SSC (mg/L)	% Annual Sediment	Days >1500 ppm	Risk Level
January	70	250	2%	0	Low
February	65	200	2%	0	Low
March	75	280	2%	0	Low
April	95	450	3%	0	Low
May	180	800	5%	1	Medium
June	350	4500	18%	25	High
July	400	5200	22%	28	High
August	380	4800	21%	27	High
September	280	2800	12%	15	Medium-High
October	150	800	4%	1	Low
November	100	400	2%	0	Low
December	70	250	2%	0	Low

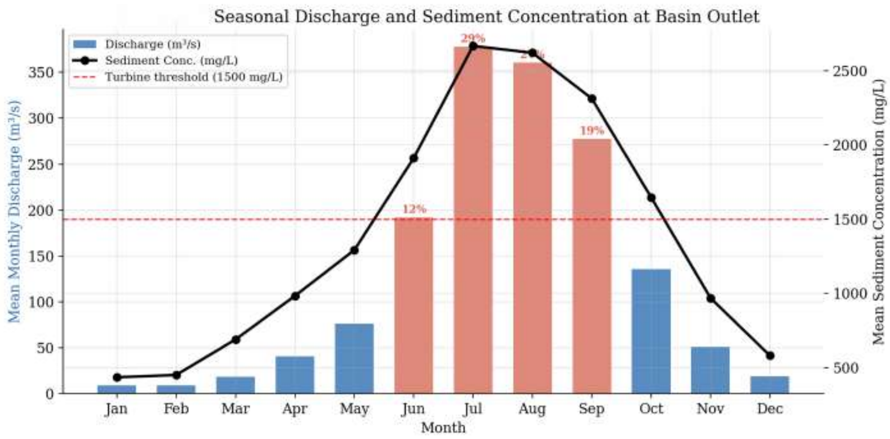

FIGURE 9. Mean monthly discharge and sediment concentration at the Marsyangdi basin outlet showing the sharp monsoon rise in sediment concentration.

With regard to hydropower operation, it becomes important to discuss the increasing SSC throughout the seasons because the sediment concentration, together with its particle size, shape, hardness, flow velocity and impingement angle determines hydro-abrasive wear of the turbine elements in sediment-rich Himalayan rivers. According to [13], despite sediment settling and flushing facilities, Nepalese run-of-river HPPs, such as Marsyangdi, Khimti, and Jhimruk operate with a high rate of turbine erosion caused by sediments. Additionally, an IHA case study of the Jhimruk HPP mentions an example of an operating rule based on the level of sediment concentration when the plant operates at full capacity below 1,500 ppm, starts to turn off the units from 1,500 to 3,000 ppm, and operates at full shut down above 3,000 ppm. Thus, according to this study, the level of exceedance of 1,500 mg/L in the outlet of Marsyangdi basin can be considered as a relevant operational criterion for periods of increased erosion risk for turbines.

Based on Table 8, this criterion is exceeded for 95 days a year, mostly in the period of June–September, accounting for 73% of the annual sediment amount. The SSC in the dry seasons does not exceed this criterion much, indicating that this is the low-risk period for turbine inspection and maintenance operations. Fig. 7 and Fig. 8 and Table 8 show that the sediment hazard in Marsyangdi basin is highly seasonal in the outlet and heterogeneous in the whole basin, and the major risk for run-of-river hydropower operation is concentrated during monsoon months [13, 14].

5. DISCUSSION

5.1. CONTROLS ON SPATIAL SEDIMENT YIELD. The spatial pattern implies that precipitation is the main factor controlling sediment production in the Marsyangdi Basin. Hotspot sub-basins occur in the wetter south of the drainage area, while northern and northwestern sub-basins exist in the dry rain shadow zone. The pattern fits the findings related to the role of monsoon forcing on hydrology and sediment delivery at the basin scale in the Himalayas [4]. Moreover, the pattern conforms to the conclusions drawn from SWAT modeling in Nepal and the Kaligandaki Basin, which states that sediment yield in this case involves complex interplay between multiple factors i.e., rainfall, topography, and channel network [5, 8].

At the same time, precipitation is not sufficient to explain the pattern. Eastern sub-basins have a significant amount of rainfall but lower sediment yield, meaning that other factors, slopes, relief and connectivity, play an important role. Therefore, one can conclude that while precipitation

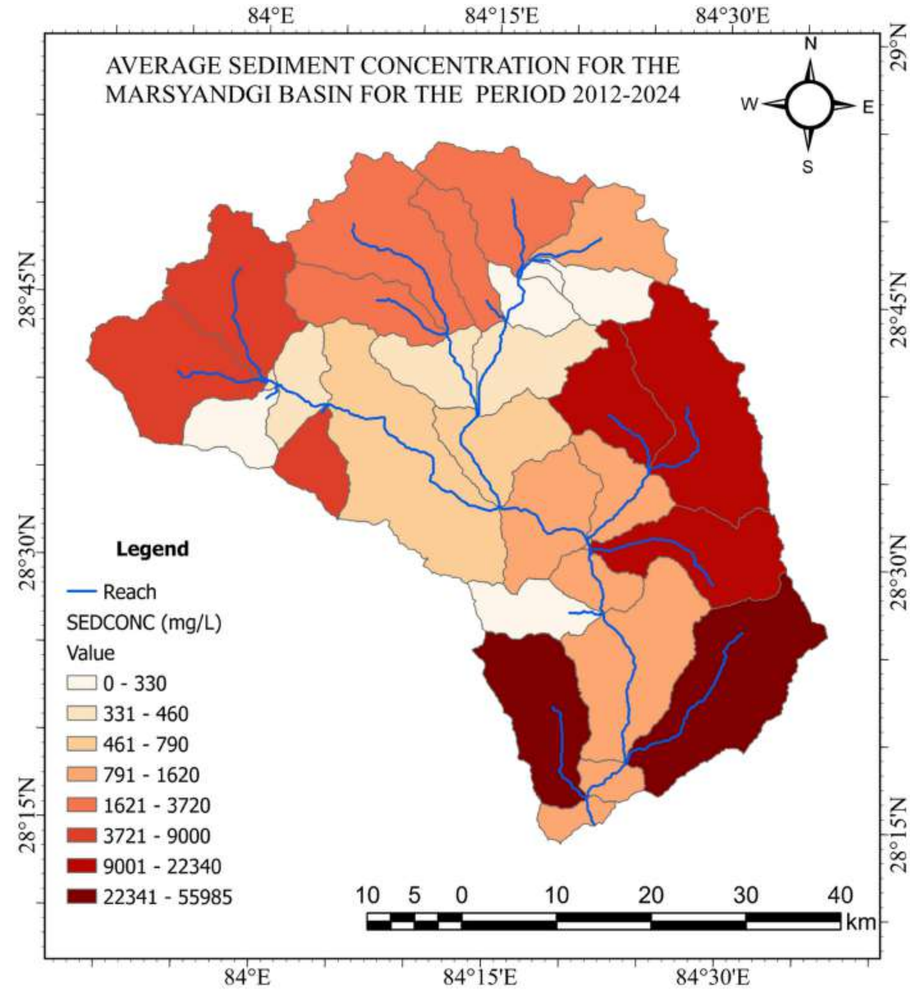

Figure 10. Spatial distribution of average sediment concentration by reach, showing pronounced spatial heterogeneity and concentration hotspots in the southern and southeastern reaches.

controls the general north-south pattern, the local intensity of sediment processes is controlled by topographic factors.

5.2. **MODEL PERFORMANCE AND UNCERTAINTY.** Performance in terms of streamflow was better than sediment, which was expected in the steep Himalayan basins considered in this research. While streamflow is representative of the entire basin's hydrology, sediment is sensitive to monsoonal rain events and to the local sediment supply. The process-based model SWAT estimates sediment yield by means of MUSLE, which simulates runoff erosion more accurately than modeling landslides, debris flow, and mass wasting events [7, 10, 15]. Hence, this could explain why the model captured the seasonal sediment cycle but smoothed out the maximum monsoon peaks.

The uncertainty in the results could stem from the limitations of the observational data used in this study. The sediment data utilized in calibration were not continuous, and the model was calibrated and validated based on one location only. Thus, while the outlet response was correctly simulated, the spatial pattern within the watershed remains an outcome of the model, without validation. Other similar studies conducted in the Himalayan area using SWAT have also reported difficulties related to uncertainty of spatial pattern resulting from one-site calibration [8]. Thus, the hot-spot sub-watersheds must be interpreted relatively rather than quantitatively.

5.3. **HYDROPOWER RELEVANCE.** In relation to hydropower plants, the key finding pertains to the temporal clustering of the sediment-related risk, which is pronounced during the monsoon period. While abrasive wear in hydropower turbines depends both on sediment concentrations and sediment grain hardness, shape, sizes and flow regime [3], the threshold used in this study can be considered only indicative.

Therefore, the current research is most useful as a basin-wide planning technique that helps to define the areas where sediment sources are clustered and the periods of the maximum sediment stress. A comparison between the sediment predictions of the model and more traditional discharge-SSC curves is needed for clarifying the added benefit of the model in this basin.

6. CONCLUSION

This study applied SWAT to estimate suspended sediment yield, sediment concentration and their spatial pattern in the Marsyangdi River Basin. SWAT can provide a useful basin-scale framework for sediment assessment in the basin as it reproduced streamflow very well and sediment with satisfactory performance. The results show that sediment yield is strongly concentrated in a small number of southern sub-basins, while the remaining sub-basins contribute relatively little. Sediment transport is also strongly seasonal with the monsoon period dominating the annual sediment regime. These findings indicate that sediment pressure in the Marsyangdi Basin is both spatially concentrated and seasonally focused.

The comparison between precipitation and sediment yield suggests that the major sediment-source areas are linked to the wetter southern part of the basin, although precipitation alone does not explain the full spatial pattern. From a practical point of view, the study helps identify where sediment-source areas are concentrated and when sediment exposure is highest. Therefore, it is useful for targeted sediment monitoring and basin-scale planning.

Part of the SSC series used in the analysis was completed using a rating-based approach because the observed sediment record was intermittent. In addition, the SWAT sediment module mainly represents runoff-driven erosion and does not explicitly simulate landslides, debris flows and other mass-wasting processes that are important in steep Himalayan catchments. The calibration and validation were also carried out at the basin outlet only, therefore the spatial sediment pattern should be read as a relative modeled pattern rather than an exact sub-basin estimate. Future work should therefore focus on improved monsoon-period sediment observations, multi-site validation, and comparison with discharge-SSC rating methods.

Acknowledgment. The authors gratefully acknowledge the Department of Hydrology and Meteorology (DHM), Nepal, for providing the hydrological and precipitation data used in this study. The authors also acknowledge the Institute of Engineering, Pulchowk Campus, for academic and institutional support. Special thanks are extended to all individuals and organizations whose data resources and technical support contributed to the completion of this work.

References

[1] B. Bookhagen, R. C. Thiede, and M. R. Strecker, "Late quaternary intensified monsoon phases control landscape evolution in the northwest himalaya," *Geology*, vol. 33, no. 2, pp. 149–152, Feb. 2005.

[2] R. K. Dahal and S. Hasegawa, "Representative rainfall thresholds for landslides in the nepal himalaya," *Geomorphology*, vol. 100, no. 3–4, pp. 429–443, Aug. 2008.

[3] L. Poudel, B. Thapa, B. P. Shrestha, B. S. Thapa, K. P. Shrestha, and N. K. Shrestha, "Computational and experimental study of effects of sediment shape on erosion of hydraulic turbines," in *IOP Conference Series: Earth and Environmental Science*, 2012.

[4] C. Andermann, S. Bonnet, A. Crave, P. Davy, L. Longuevergne, and R. Gloaguen, "Sediment transfer and the hydrological cycle of himalayan rivers in nepal," *Comptes Rendus - Geoscience*, vol. 344, no. 11–12, pp. 627–635, Nov. 2012.

[5] P. Chinnasamy and A. Sood, "Estimation of sediment load of kaligandaki basin," *Journal of Earth System Science*, May 2020.

[6] J. G. Arnold *et al.*, "Swat: Model use, calibration, and validation," *Transactions of the ASABE*, vol. 55, no. 4, pp. 1491–1508, 2012. [Online]. Available: http://swatmodel.tamu.edu

[7] P. W. Gassman, M. R. Reyes, C. H. Green, and J. G. Arnold, "The soil and water assessment tool: Historical development, applications, and future research directions," *Transactions of the ASABE*, vol. 50, no. 4, pp. 1211–1250, 2007.

[8] B. Dhami, S. K. Himanshu, A. Pandey, and A. K. Gautam, "Evaluation of the swat model for water balance study of a mountainous snowfed river basin of nepal," *Environmental Earth Sciences*, vol. 77, no. 1, Jan. 2018.

[9] S. Ghimire, U. Singh, and P. K. Bhattarai, "Generation of a suspended sediment rating curve of a himalayan river based on a long-term data: A case study of kabeli river," in *IOE Graduate Conference*, no. 10, Aug. 2021, pp. 2350–8906.

[10] S. L. Neitsch, J. G. Arnold, J. R. Kiniry, and J. R. Williams, "Soil and water assessment tool theoretical documentation: Version 2009," Texas Water Resources Institute, Texas A&M University, Tech. Rep., 2011. [Online]. Available: https://www.researchgate.net/publication/306205252_Soil_and_water_asessment_tool_theoritical_documentation_version_2009_Texas_Water_Resources_Institute_technical_report_No_406_Texas_Water_Resources_Institute_Texas_AM_University_Texas

[11] K. C. Abbaspour, E. Rouholahnejad, S. Vaghefi, R. Srinivasan, H. Yang, and B. Kløve, "A continental-scale hydrology and water quality model for europe: Calibration and uncertainty of a high-resolution large-scale swat model," *Journal of Hydrology*, vol. 524, pp. 733–752, May 2015.

[12] T. P. Joshi and B. K. Mishra, "Assessment of run-of-river hydropower potential using swat modeling and gis in the marsyangdi river basin, nepal," *Journal of Hydrology and Meteorology*, vol. 12, no. 1, pp. 11–22, Dec. 2024.

[13] B. Thapa, R. Shrestha, P. Dhakal, and B. S. Thapa, "Problems of nepalese hydropower projects due to suspended sediments," *Aquatic Ecosystem Health and Management*, vol. 8, no. 3, pp. 251–257, Jul. 2005.

[14] International Hydropower Association, "Sediment management case studies, nepal - jhimruk," Jul. 2026, accessed: 2026-07-06. [Online]. Available: https://www.hydropower.org/sediment-management-case-studies/nepal-jhimruk

[15] J. G. Arnold *et al.*, "Swat: Model use, calibration, and validation," *Transactions of the ASABE*, vol. 55, no. 4, pp. 1491–1508, 2012. [Online]. Available: http://swatmodel.tamu.edu